Molecular Pharmacology Fast Forward. Published on February 29, 2012 as doi:10.1124/mol.112.077693
This article has not been copyedited and formatted. The final version may differ from this version.

Non-equilibrium activation of a G-protein-coupled receptor

Manuela Ambrosio and Martin J. Lohse

Institute of Pharmacology and Toxicology, University of Würzburg, Germany

Institute of Pharmacology and Toxicology

Versbacher Straße 9

D-97078 Würzburg, Germany

Molecular Pharmacology Fast Forward. Published on February 29, 2012 as DOI: 10.1124/mol.112.077693
This article has not been copyedited and formatted. The final version may differ from this version.

Running title:

Non-equilibrium α_{2A}-adrenergic receptor activation

Corresponding author:

M.J. Lohse, Institute of Pharmacology and Toxicology, Versbacher Straße 9, D-97078 Würzburg, Germany. lohse@toxi.uni-wuerzburg.de

31 text pages

6 figures

2 tables

41 references

248 words in the Abstract

746 words in the Introduction

1,346 words in the Discussion

Molecular Pharmacology Fast Forward. Published on February 29, 2012 as DOI: 10.1124/mol.112.077693
This article has not been copyedited and formatted. The final version may differ from this version.

Abbreviations:

GPCR, G-protein coupled receptor

α_{2A}-AR, α_{2A}-adrenergic receptor

NE, norepinephrine

FRET, fluorescence resonance energy transfer

FlAsH, fluorescein arsenical hairpin binder

YFP, yellow fluorescent protein

CFP, cyan fluorescent protein

HEK, human embryonic kidney

EDT, ethanedithiol

DMEM, Dulbecco's modified Eagle's medium

Molecular Pharmacology Fast Forward. Published on February 29, 2012 as DOI: 10.1124/mol.112.077693
This article has not been copyedited and formatted. The final version may differ from this version.

Abstract

G-protein coupled receptor activation is generally analyzed under equilibrium conditions. However, real-life receptor functions are often dependent on very short and transient stimuli that may not allow the achievement of the steady state. This is particularly true for synaptic receptors like the α_{2A}-adrenergic receptor (AR). Therefore, we recently developed a fluorescence resonance energy transfer based technology to study non-equilibrium α_{2A}-AR function in living cells. To examine the effects of increasing concentrations of the endogenous agonist norepinephrine on the speed and extent of α_{2A}-AR activation with very high temporal resolution, we took advantage of an α_{2A}-$AR^{FlAsH/CFP}$ sensor. The results indicate that the efficacy of norepinephrine in eliciting receptor activation increased in a time-dependent way reaching the maximum with a half-life of ≈60 ms. The EC_{50}-values under non-equilibrium conditions start at ≈26 μM (t=40 ms) and show a 10-fold decrease until the steady-state is achieved. To analyze norepinephrine ability in triggering a downstream intracellular response after α_{2A}-AR stimulation, we monitored the kinetics and amplitude of G_i activation in real time using a $G_i^{CFP/YFP}$ sensor. The results show that both the efficacy and the potency of norepinephrine in inducing G_i activation achieve a steady-state slower compared to receptor activation, and that the initial EC_{50}-value of ≈100 nM decreases in an exponential way reaching the minimal value ≈10 nM at equilibrium. Thus, both efficacy and potency of norepinephrine increased about 10-fold over a few seconds of agonist stimulation, illustrating that receptor and G-protein signaling as well as signal amplification are highly time-dependent phenomena.

Molecular Pharmacology Fast Forward. Published on February 29, 2012 as DOI: 10.1124/mol.112.077693
This article has not been copyedited and formatted. The final version may differ from this version.

Introduction

G-protein-coupled receptors (GPCRs) represent the largest family of membrane receptors for a big number of diverse endogenous ligands, including hormones and neurotransmitters (Lefkowitz, 2000). The binding of an extracellular agonist to its receptor represents the initial step in the signaling pathway and has been classically investigated by radioligand binding experiments. Those studies allow the determination of equilibrium affinities (K_i- and K_D-values) and also give important details about ligand association/dissociation rates at the receptor level (Hulme and Trevethick, 2010). However, such experiments require long incubation times (from several minutes to hours) and, thus, cannot represent a real-time approach. Furthermore, binding studies are limited to the interaction between ligands and receptors and cannot explore the activation of the receptor once it is bound to an agonist. After the binding of an extracellular agonist to its GPCR, the signaling pathway proceeds with the receptor switching from a resting state into an active conformation that allows the binding and activation of the cognate G-proteins and, hence, the transduction of a transmembrane signal to the downstream effectors (e.g. adenylyl cyclases, phospholipases, ion channels). Because until recently the agonist-induced receptor conformational rearrangements were not directly accessible, GPCR activation was traditionally inferred from the stimulation of a receptor-mediated downstream biological response that could be easily measured experimentally. Together with the binding assays, such activation assays have led to the classical concepts of receptor theory. Most methods applied for these studies do not use intact cells and are usually performed under equilibrium conditions needing extended incubation times that do not allow a continuous, real-time monitoring of receptor activity. However, under physiological conditions, both receptor

Molecular Pharmacology Fast Forward. Published on February 29, 2012 as DOI: 10.1124/mol.112.077693
This article has not been copyedited and formatted. The final version may differ from this version.

binding and activation are often dependent on very short stimuli and usually do not reach the steady state. This is especially true for receptors involved in synaptic transmission, like α_{2A}-ARs. These rhodopsin-like GPCRs mediate the biological effects of endogenous catecholamines, most notably in presynaptic control of neurotransmitter release, thus playing a key role in the modulation of many physiological functions of the sympathetic nervous system (Hein, 2006; Philipp and Hein, 2004). Norepinephrine is the principal neurotransmitter of postganglionic sympathetic nerves. Once released, it diffuses across the synaptic space and exerts its function by binding and activating either presynaptic α_{2A}-ARs on the nerve ending or postsynaptic α_{2A}-ARs on the effector organ. Recently, fast cyclic voltammetry measurements in multiple brain regions have shown that the maximal evoked norepinephrine release in vivo is in the micromolar range and that the time required for the overflow to decay to half of the maximum is a few seconds (Park et al., 2009; Park et al., 2011).

Because the physiological dynamics of norepinephrine are not compatible with the classic approaches applied to detect receptor activation, we developed a technology to study non-equilibrium α_{2A}-AR function in real time. The recent development of optical techniques that permit the study of GPCR-mediated signaling processes in intact cells, facilitates the analysis of distinct signaling steps in a more physiological setting (reviewed by (Lohse et al., 2008b)). Taking advantage of a fluorescence resonance energy transfer (FRET)-based approach, it is possible to follow the conformational changes of GPCRs in living cells and gain information about the characteristics and kinetics of GPCR activation in real time (Vilardaga et al., 2003). Placement of a donor (e.g. cyan fluorescent protein, CFP) and an acceptor fluorophore (e.g. the small fluorescein arsenical hairpin binder FlAsH) into the third intracellular loop and at the C-

Molecular Pharmacology Fast Forward. Published on February 29, 2012 as DOI: 10.1124/mol.112.077693
This article has not been copyedited and formatted. The final version may differ from this version.

terminus, respectively, led to the development of an α_{2A}-AR sensor (Figure 1) whose activation can be measured by recording intramolecular FRET. Kinetic measurements have previously suggested that, given enough receptors and G-proteins, the receptor-G-protein interaction occurs as fast as receptor activation itself, therefore not representing a time-limiting step in the signaling pathway (Hein et al., 2005; Hein et al., 2006). In contrast, the subsequent G-protein activation limits the progression of the receptor-mediated signaling cascade (Bünemann et al., 2003; Hein et al., 2006; Jensen et al., 2009): even though receptor-G-protein interaction is already maximal after ≈50 ms, at this point only a small fraction of G-protein is activated, and it takes ≈1-2 s until the G-protein activation reaches its maximum.

These new techniques allow the study of receptor activation and signaling and thus the investigation of potencies and efficacies under non-equilibrium conditions. Here, taking advantage of both receptor and G-protein FRET-based sensors, we analyzed the norepinephrine-induced α_{2A}-AR activation under such non-equilibrium conditions. This approach allowed the real-time monitoring of norepinephrine-mediated effects occurring in the millisecond time scale in living cells, thus reflecting the physiological synaptic events.

Molecular Pharmacology Fast Forward. Published on February 29, 2012 as DOI: 10.1124/mol.112.077693
This article has not been copyedited and formatted. The final version may differ from this version.

Materials and Methods

Materials. Norepinephrine (NE) was obtained from Sigma (St. Louis, MO). FlAsH is commercially available from Invitrogen (Carlsbad, CA) as TC-FlAsH.

Cell culture and transfection. Cells were seeded on round polylysine-coated coverslips that were placed in six-well plates and maintained in Dulbecco's modified Eagle's medium supplemented with 10% fetal calf serum and 100,000 U/liter penicillin and 100 mg/liter streptomycin at 37 °C in 7% CO_2. HEK-293 cells stably expressing α_{2A}-AR$^{FlAsH/CFP}$ (Hoffmann et al., 2005) have been previously described (Nikolaev et al., 2006). HEK-293 cells were transfected with the plasmids encoding the wild-type α_{2A}-AR and the heterotrimeric $G_i^{CFP/YFP}$ sensor (Bünemann et al., 2003) using Effectene (Qiagen, Hilden, Germany). The amount of cDNA used for the transient transfection of the wild-type α_{2A}-AR was chosen to give overall a similar receptor expression (~2 pmol/mg) as determined by radioligand binding experiments.

FlAsH-labeling. The FlAsH-labeling was performed as previously described (Hoffmann et al., 2005; Hoffmann et al., 2010). Briefly, α_{2A}-AR$^{FlAsH/CFP}$ expressing HEK-293 cells were washed twice with Phenol Red-free Hanks' balanced salt solution containing 1 g/liter glucose (HBSS; Invitrogen) and subsequently incubated with 500 nM FlAsH suspended in HBSS containing 12.5 μM 1,2-ethanedithiol (EDT) for 1 h at 37 °C. To reduce nonspecific labeling, cells were washed with HBSS, incubated at 37 °C for 10 min with HBSS containing 250 μM EDT, and again rinsed twice with HBSS before being used for fluorescence measurements. We have shown earlier that this labeling procedure does not interfere with the kinetic properties of the labeled receptors (Hoffmann et al., 2005).

Molecular Pharmacology Fast Forward. Published on February 29, 2012 as DOI: 10.1124/mol.112.077693
This article has not been copyedited and formatted. The final version may differ from this version.

Fluorescence measurements. FRET experiments were performed in whole cells as previously described (Hoffmann et al., 2005; Maier-Peuschel et al., 2010; Nikolaev et al., 2006; Reiner et al., 2010; Vilardaga et al., 2003; Vilardaga et al., 2005; Zürn et al., 2009). In brief, transfected cells grown on coverslips were washed with HBSS and maintained in buffer A (140 mM NaCl, 5 mM KCl, 2 mM $CaCl_2$, 1 mM $MgCl_2$, and 10 mM HEPES, pH 7.3) at room temperature. Coverslips were mounted on an Attofluor holder (Invitrogen) and placed on a Zeiss inverted microscope (Axiovert 135; Carl Zeiss, Jena, Germany) equipped with an oil immersion 100× objective and a dual-emission photometric system (Till Photonics, Gräfelfing, Germany). Samples were excited with light from a polychrome IV (Till Photonics). To both minimize photobleaching and enable fast temporal resolution the illumination and recording times were set to 14-40 ms and 20-100 ms respectively. FRET was monitored as the emission ratio of FlAsH or YFP to CFP, F_{535}/F_{480}, where F_{535} and F_{480} are the emission intensities at 535 ± 15 nm and 480 ± 20 nm (beam splitter DCLP 505 nm) upon excitation at 436 ± 10 nm (beam splitter DCLP 460 nm). Special care was taken to ensure similar fluorescence levels and distribution in the examined cells. The emission ratio was corrected by the respective spillover of CFP into the 535 nm channel (spillover of FlAsH and YFP into the 480 nm channel was negligible) to give a corrected ratio F^*_{535}/F^*_{480}. The FlAsH (or YFP) emission upon excitation at 480 nm was recorded for each experiment to subtract direct excitation from the corrected ratio. To determine agonist-induced changes in FRET, cells were continuously superfused with buffer A, and single concentrations of norepinephrine were applied using a computer-assisted solenoid valve-controlled rapid superfusion device ALA-VM8 (ALA Scientific Instruments, Westbury, NY; solution exchange, 5-10 ms). Signals detected by

Molecular Pharmacology Fast Forward. Published on February 29, 2012 as DOI: 10.1124/mol.112.077693
This article has not been copyedited and formatted. The final version may differ from this version.

avalanche photodiodes were digitized using an AD converter (Digidata 1322A; Molecular Devices, Sunnyvale, CA) and stored on a personal computer using Clampex 8.1 software (Molecular Devices). The agonist-induced decrease in FRET ratio was fitted to the equation: $A(t) = A_0 - A_1 \times e^{-t/\tau}$, where τ is the time constant (ms), and A is the amplitude of the signal.

Molecular Pharmacology Fast Forward. Published on February 29, 2012 as DOI: 10.1124/mol.112.077693
This article has not been copyedited and formatted. The final version may differ from this version.

Results

To investigate the effects of different concentrations of the full agonist norepinephrine on the speed and extent of α_{2A}-AR activation in real time, we used a FRET approach taking advantage of the fully functional α_{2A}-AR$^{FlAsH/CFP}$ FRET sensor (Figure 1A) (Hoffmann et al., 2005; Nikolaev et al., 2006). HEK-293 cells expressing the receptor construct were labeled with FlAsH, and single cells were monitored under a microscope for CFP and FlAsH fluorescence as described under *Materials and Methods*. To detect changes in FRET with very high temporal resolution, we illuminated single cells with 14 ms pulses with a frequency of 50 Hz at 436 nm. In agreement with earlier data, superfusion with saturating concentrations of norepinephrine (NE, 1 mM) resulted in a rapid decrease of the FRET signal (F^*_{FlAsH}/F^*_{CFP}) due to the simultaneous increase in the CFP fluorescence and decrease in the FlAsH fluorescence (Figure 1A, *right*). This FRET change reveals the full agonist-induced receptor activation and typically occurs in a millisecond time scale (Vilardaga et al., 2003). The maximal FRET response was high ($\Delta F^*_{FlAsH}/F^*_{CFP} \approx 20\%$), therefore the superfusion of the cells even with low concentrations of norepinephrine produced FRET responses with a high signal to noise ratio. Figure 2A shows that stimulation with increasing concentrations of the agonist (NE, 1 μM – 1 mM) led to correspondingly increasing FRET signals (as a reference for full receptor activation for each experiment the response was normalized to the effects of norepinephrine 1 mM at $t > 2$ s). In addition, the time to the half-maximal FRET response was variable and depended on the degree of receptor activation, with a saturation value for the rate constant of ≈60 ms, achieved at high agonist concentrations (Figure 2B).

Molecular Pharmacology Fast Forward. Published on February 29, 2012 as DOI: 10.1124/mol.112.077693
This article has not been copyedited and formatted. The final version may differ from this version.

Because the FRET-based approach applied here represents a unique tool to monitor the receptor conformational changes in real time, we were able to determine the speed and the extent of the agonist-induced receptor activation every 20 ms. Using those FRET data, we established a pool of time-dependent concentration-response curves (a selection is shown in Figure 3) that show EC_{50}-values (i.e. effective norepinephrine concentrations evoking 50% of the maximal response) that clearly moved to the left over time until the steady state was achieved (< 2 s; see Table 1). Similar to the potency, also the efficacy of norepinephrine in eliciting α_{2A}-$AR^{FlAsH/CFP}$ activation rose in a time-dependent way and then reached a saturation value (set to 100%).

In order to analyze in real time the ability of increasing concentrations of norepinephrine to produce a downstream intracellular response after α_{2A}-AR stimulation, we analyzed the kinetics and the amplitude of G_i-activation in single intact cells. To this purpose, we transfected HEK-293 cells expressing the α_{2A}-AR with the previously well characterized $G_i^{CFP/YFP}$ sensor consisting of the three subunits $G\alpha_i^{YFP}$, $G\beta$ and $G\gamma^{CFP}$ (Figure 1B) (Bünemann et al., 2003). As previously shown, stimulation with saturating concentration of norepinephrine triggers a robust FRET decrease ($\Delta F^*_{YFP}/F^*_{CFP}$), which is significantly slower compared to the maximal speed of receptor activation (Figure 1B, *right*). Figure 4 represents the time-resolved FRET changes of G_i-activation induced by norepinephrine concentrations ranging from 1 nM up to 1 mM. For each experiment, the FRET change was normalized to the maximal effect achieved by saturating concentrations of norepinephrine. In agreement with data published before (Bünemann et al., 2003), the amplitude of G_i activation achieved maximal values only at higher agonist concentrations (Figure 4A). Similarly, also the speed of G_i activation increased with increasing concentrations of norepinephrine,

Molecular Pharmacology Fast Forward. Published on February 29, 2012 as DOI: 10.1124/mol.112.077693
This article has not been copyedited and formatted. The final version may differ from this version.

reaching the minimal value of ≈600 ms at saturating concentrations of the agonist (Figure 4B). In order to investigate how the potency and the efficacy of norepinephrine in triggering G_i-activation change under non-equilibrium conditions, we developed a series of concentration-response curves of G_i-activation, starting with the FRET data recorded 100 ms after agonist superfusion and proceeding every 100 ms until the steady-state was reached. As shown in Figure 5, both the potency and the efficacy of norepinephrine at the G-protein level highly depended on time and reached the maximum values solely under equilibrium conditions ($t > 10$ s). The changes in potency were best seen from the decreases in the EC_{50}-values given in Table 2.

A comparison of the time-dependent norepinephrine-mediated effects at the α_{2A}-AR and at the G_i-protein level is summarized in Figure 6. As shown, the efficacy of norepinephrine at the receptor level reached its maximum with an apparent half-life of 58 ± 3 ms (Figure 6A), whereas at the G_i-protein level the E_{max}-values followed a two-phase kinetics with a faster and a slower component (half-life$_1$ = 128 ± 60 ms and half-life$_2$ = 658 ± 40 ms). The top panel in Figure 6B shows the time-dependent potency of norepinephrine at the receptor level: the EC_{50}-values decreased with a half-life of 330 ± 11 ms, starting at ≈26 μM (40 ms after norepinephrine superfusion) and reaching ≈2 μM at steady state. As depicted in Figure 6B (bottom panel), the EC_{50}-values relative to G_i-activation also decreased in a time-dependent manner, but reached the steady-state with a half-life of 2,520 ± 168 ms. The potency of the full agonist norepinephrine in eliciting G_i-activation started at ≈100 nM after a 100 ms pulse of norepinephrine and increased exponentially until the equilibrium was achieved. In the latter condition the EC_{50}-value was ≈10 nM.

Molecular Pharmacology Fast Forward. Published on February 29, 2012 as DOI: 10.1124/mol.112.077693
This article has not been copyedited and formatted. The final version may differ from this version.

The relationship between the potency of norepinephrine at the receptor and at the G-protein level is represented in Figure 6C and indicates a large time-dependent amplification of the agonist-induced signal at the α_{2A}-AR.

Molecular Pharmacology Fast Forward. Published on February 29, 2012 as DOI: 10.1124/mol.112.077693
This article has not been copyedited and formatted. The final version may differ from this version.

Discussion

Classic receptor theory is largely based on in vitro measurements in which the receptor is exposed to a constant concentration of ligand under steady-state conditions (Clark, 1933; Black et al., 1985; Kenakin, 2002; Molinoff et al., 1981; Weiland and Molinoff, 1981). Because a failure to attain equilibrium would lead to an underestimation of ligand binding and receptor activation ability, these studies usually require long incubation times (Hulme and Trevethick, 2010). Both the theory and experimental data on the kinetics of ligand binding to receptors indicate that these processes depend on ligand concentration (see e.g. (Hulme and Trevethick, 2010).

Accordingly, these assay conditions only poorly mimic the temporal concentrations and duration of exposure that the agonist exerts against its target in an in vivo setting. In fact, under physiological conditions, i.e. in response to nerve activity, stimulation of α_{2A}-AR may be very short-lived, but in response to high agonist concentrations. For example, it has been estimated that in neurovascular junctions, norepinephrine concentrations might be in excess of 100 μM, but for times as short as only 100 ms (Bevan et al., 1987; Bevan et al., 1984). These short stimulation pulses with high norepinephrine concentrations result from its rapid release from vesicles where its concentrations can exceed several hundred mM, followed by rapid reuptake (Philippu and Matthaei, 1988). However, to date no techniques were available to either assess ligand binding with sufficient speed or to assess the resultant receptor activation itself in real time – with the exception of the ion channel receptors where a lot of kinetic experiments and theories have been done notably by Colquhoun and colleagues (Colquhoun, 2007).

In order to study the characteristics and kinetics of GPCR activation in a more native

Molecular Pharmacology Fast Forward. Published on February 29, 2012 as DOI: 10.1124/mol.112.077693
This article has not been copyedited and formatted. The final version may differ from this version.

environment, we have recently developed a FRET-based approach, which enables the detection of the fast activation speed of the receptors and their cognate G-proteins in intact cells (Lohse et al., 2008a). Here, taking advantage of those FRET-based sensors, we were able to monitor the non-equilibrium α_{2A}-AR function in living HEK-293 cells. The time-resolved analysis of the norepinephrine-induced FRET signals recorded from single HEK-293 cells expressing the α_{2A}-AR$^{FlAsh/CFP}$ sensor are in agreement with earlier studies (Hoffmann et al., 2005; Vilardaga et al., 2003; Vilardaga et al., 2005). First, they confirm that the FRET-signal extent is proportional to the superfused concentration of agonist, with saturating concentrations of norepinephrine triggering the maximal FRET decrease (Figure 2A). Next, they support the notion that the speed of receptor activation highly depends on agonist concentrations, with higher concentrations of norepinephrine triggering FRET changes more rapidly until a saturation value of ≈60 ms is reached; this value presumably represents the upper limit of the true activation time of the α_{2A}-AR (Figure 2B).

The high FRET responses and the high signal to noise ratio characterizing the α_{2A}-AR$^{FlAsh/CFP}$ sensor allowed us to monitor the agonist-dependent receptor activation with very high temporal resolution, recording the fluorescence emissions of the donor and the acceptor fluorophores every 20 ms. Thus, we were able to establish a pool of concentration-response curves under non-equilibrium conditions (Figure 3). As expected, the efficacy of norepinephrine in eliciting α_{2A}-AR$^{FlAsH/CFP}$ activation rose in a time-dependent way and reached its maximum with an apparent half-life of ≈60 ms (Figure 6A). As represented in Figure 6B (top panel), the corresponding EC_{50}-values decreased in an exponential manner reaching ≈2 μM at steady state. The equilibrium EC_{50}-value of 2 μM is high compared with potencies determined in other types of

Molecular Pharmacology Fast Forward. Published on February 29, 2012 as DOI: 10.1124/mol.112.077693
This article has not been copyedited and formatted. The final version may differ from this version.

functional experiments, but it is similar to the affinity of the low-affinity state of the α_{2A}-AR, which we previously determined performing radioligand binding experiments with cell membranes (Nikolaev et al., 2006; Vilardaga et al., 2003). It most likely represents the true affinity of the receptor itself in intact cells, i.e. in the non-G-protein-bound state. These observations correlate well with the apparent lack of a "receptor reserve" when receptor activation itself was monitored in intact cells.

In the GPCR signaling pathway, the interaction of an agonist-activated receptor with the cognate G-protein results in the activation of the G-protein. Therefore, in order to evaluate α_{2A}-AR activation through a receptor-mediated downstream biological response, we took advantage of a $G_i^{CFP/YFP}$ sensor, which allows a direct real-time measurement of G_i-activation. The $G_i^{CFP/YFP}$ sensor gives rise to FRET responses showing relatively high signal to noise ratios that allow the recording of the FRET values every 100 ms. As expected, the amplitude of the FRET changes depended on agonist concentrations and the time courses of G_i-activation reached maximal values only at high norepinephrine concentrations (Figure 4). The ≈10 times slower speed of G_i-activation compared to receptor activation itself is in agreement with earlier data, which suggest that G-protein activation is the rate-limiting step in the activation of the signaling cascade (Hein et al., 2005; Hein et al., 2006). The development of non-equilibrium concentration-response curves using the FRET data of G_i-activation confirms that with our FRET-based approach in intact cells, we can experimentally reproduce the classic receptor theory predictions. As depicted in Figure 6A, the efficacy of norepinephrine in activating the cognate G_i-protein increased until equilibrium was achieved. Here, in contrast to the receptor activation kinetics, the E_{max}-values followed a two-phase kinetics that very well agrees with the notion that after the rapid G-protein

Molecular Pharmacology Fast Forward. Published on February 29, 2012 as DOI: 10.1124/mol.112.077693
This article has not been copyedited and formatted. The final version may differ from this version.

recruitment to the activated receptor, a slow step – probably the GDP release from the G-protein – limits the G-protein activation speed, thus making it the time-limiting step of the signaling cascade (Hein et al., 2006). As shown in Figure 6B (bottom panel), the EC_{50}-values for G_i-activation decreased in a time-dependent manner and reached the steady-state ≈8 times slower than shown above for the activation of the receptor. The equilibrium EC_{50}-value of the full agonist norepinephrine in eliciting G_i-activation was ≈10 nM in accordance with a high degree of receptor reserve existing in our transfected cell system and corresponding to the presence of a large receptor reserve identified in electrophysiological studies with transfected cells (Bünemann et al., 2001).

A comparison of the two panels in Figure 6B reveals the differences in norepinephrine required to elicit half-maximal responses for the receptor itself or for G_i. As shown in Figure 6C, these data illustrate that over short stimulation phases, the amplification between receptors and G-proteins first becomes smaller – as receptors initially activate faster than G_i -, but then continues to increase until it achieves 2.5 orders of magnitude. This large amplification demonstrates a large "receptor reserve", which means that only a fraction of the receptors available on the cell membrane needs to be activated to generate a maximal downstream signaling effect (Ariens et al., 1960; Nickerson, 1956). This concept has been much discussed on the basis of various types of analyses of neurotransmitter release experiments (Agneter et al., 1993; Agneter et al., 1997). Many biological systems involving α_{2A}-adrenergic receptors have been reported to display a large receptor reserve, including presynaptic control of neurotransmitter release in various brain regions (Adler et al., 1987), prejunctional receptors at the *Vas deferens* (Sallés et al., 1994), receptors on human platelets (Lenox et al., 1985), receptors controlling venous (but not arterial) tone (Ruffolo, 1986) as well as receptors

Molecular Pharmacology Fast Forward. Published on February 29, 2012 as DOI: 10.1124/mol.112.077693
This article has not been copyedited and formatted. The final version may differ from this version.

controlling behavioural and physiological responses (Durcan et al., 1994).

Our data now show that the signal amplification underlying the receptor reserve is time-dependent, and increases in our case over a period of ≈15 s by almost one order of magnitude.

In conclusion, the high temporal resolution achieved with our FRET-based technology was successfully applied to monitor norepinephrine-mediated effects on α_{2A}-AR activation and signaling in real time. Taken together, our experimental findings reflect well the physiological synaptic events and look like the theoretical predictions of classic receptor theory, which postulate that under non-equilibrium conditions higher agonist concentrations are required to achieve receptor binding and activation (Convents et al., 1987; Severne et al., 1987). Thus, over stimulation times of less than a second, agonist potency as well as efficacy at the receptor increase, followed by similar increases at the level of G_i, occurring over a few seconds. Receptor-mediated signaling as well as signal amplification are, therefore, highly dependent on stimulation times. This adds another level of complexity to agonist effects at G-protein-coupled receptors.

Molecular Pharmacology Fast Forward. Published on February 29, 2012 as DOI: 10.1124/mol.112.077693
This article has not been copyedited and formatted. The final version may differ from this version.

Authorship Contributions

Participated in research design: Ambrosio, Lohse

Conducted experiments: Ambrosio

Contributed new reagents or analytic tools: ---

Performed data analysis: Ambrosio

Wrote or contributed to the writing of the manuscript: Ambrosio, Lohse

References

Adler CH, Meller E and Goldstein M (1987) Receptor reserve at the alpha-2 adrenergic receptor in the rat cerebral cortex. *J Pharmacol Exp Ther* **240**(2):508-515.

Agneter E, Drobny H and Singer EA (1993) Central α_2-autoreceptors: agonist dissociation constants and recovery after irreversible inactivation. *Br J Pharmacol* **108**(2):370-375.

Agneter E, Singer EA, Sauermann W and Feuerstein TJ (1997) The slope parameter of concentration-response curves used as a touchstone for the existence of spare receptors. *Naunyn Schmiedebergs Arch Pharmacol* **356**(3):283-292.

Ariens EJ, van RJ and Koopman PC (1960) Receptor reserve and threshold phenomena. I. Theory and experiments with autonomic drugs tested on isolated organs. *Arch Int Pharmacodyn Ther* **127**:459-478.

Bevan JA, Laher I and Rowan R (1987) Some implications of the high intrasynaptic norepinephrine concentrations in resistance arteries. *Blood Vessels* **24**(3):137-140.

Bevan JA, Tayo FM, Rowan RA and Bevan RD (1984) Presynaptic alpha-receptor control of adrenergic transmitter release in blood vessels. *Fed Proc* **43**(5):1365-1370.

Black JW, Leff P, Shankley NP and Wood J (1985) An operational model of pharmacological agonism: the effect of E/[A] curve shape on agonist dissociation constant estimation. *Br J Pharmacol* **84**(2):561-571.

Bünemann M, Bucheler MM, Philipp M, Lohse MJ and Hein L (2001) Activation and deactivation kinetics of α_{2A}- and α_{2C}-adrenergic receptor-activated G protein-

activated inwardly rectifying K^+ channel currents. *J Biol Chem* **276**(50):47512-47517.

Bünemann M, Frank M and Lohse MJ (2003) G_i protein activation in intact cells involves subunit rearrangement rather than dissociation. *Proc Natl Acad Sci U S A* **100**(26):16077-16082.

Clark AJ. London: E Arnold Company; 1933. The Mode of Action of Drugs on Cells.

Colquhoun D (2007) What have we learned from single ion channels? *J Physiol* **581**(Pt 2):425-427.

Convents A, De Backer JP, Convents D and Vauquelin G (1987) Tight agonist binding may prevent the correct interpretation of agonist competition binding curves for α_2-adrenergic receptors. *Mol Pharmacol* **32**(1):65-72.

Durcan MJ, Morgan PF, Van Etten ML and Linnoila M (1994) Covariation of α_2-adrenoceptor density and function following irreversible antagonism with EEDQ. *Br J Pharmacol* **112**(3):855-860.

Hein L (2006) Adrenoceptors and signal transduction in neurons. *Cell Tissue Res* **326**(2):541-551.

Hein P, Frank M, Hoffmann C, Lohse MJ and Bünemann M (2005) Dynamics of receptor/G protein coupling in living cells. *EMBO J* **24**(23):4106-4114.

Hein P, Rochais F, Hoffmann C, Dorsch S, Nikolaev VO, Engelhardt S, Berlot CH, Lohse MJ and Bünemann M (2006) Gs activation is time-limiting in initiating receptor-mediated signaling. *J Biol Chem* **281**(44):33345-33351.

Hoffmann C, Gaietta G, Bünemann M, Adams SR, Oberdorff-Maass S, Behr B, Vilardaga JP, Tsien RY, Ellisman MH and Lohse MJ (2005) A FlAsH-based

FRET approach to determine G protein-coupled receptor activation in living cells. *Nat Methods* **2**(3):171-176.

Hoffmann C, Gaietta G, Zürn A, Adams SR, Terrillon S, Ellisman MH, Tsien RY and Lohse MJ (2010) Fluorescent labeling of tetracysteine-tagged proteins in intact cells. *Nat Protoc* **5**(10):1666-1677.

Hulme EC and Trevethick MA (2010) Ligand binding assays at equilibrium: validation and interpretation. *Br J Pharmacol* **161**(6):1219-1237.

Jensen JB, Lyssand JS, Hague C and Hille B (2009) Fluorescence changes reveal kinetic steps of muscarinic receptor-mediated modulation of phosphoinositides and Kv7.2/7.3 K^+ channels. *J Gen Physiol* **133(**4):347-359.

Kenakin T (2002) Efficacy at G-protein-coupled receptors. *Nat Rev Drug Discov* **1**(2):103-110.

Lefkowitz RJ (2000) The superfamily of heptahelical receptors. *Nat Cell Biol* **2(**7):E133-136.

Lenox RH, Ellis J, Van Riper D and Ehrlich YH (1985) Alpha 2-adrenergic receptor-mediated regulation of adenylate cyclase in the intact human platelet. Evidence for a receptor reserve. *Mol Pharmacol* **27**(1):1-9.

Lohse MJ, Hein P, Hoffmann C, Nikolaev VO, Vilardaga JP and Bünemann M (2008a) Kinetics of G-protein-coupled receptor signals in intact cells. *Br J Pharmacol* **153 Suppl 1**:S125-132.

Lohse MJ, Nikolaev VO, Hein P, Hoffmann C, Vilardaga JP and Bünemann M (2008b) Optical techniques to analyze real-time activation and signaling of G-protein-coupled receptors. *Trends Pharmacol Sci* **29**(3):159-165.

Maier-Peuschel M, Frölich N, Dees C, Hommers LG, Hoffmann C, Nikolaev VO and Lohse MJ (2010) A fluorescence resonance energy transfer-based M2 muscarinic receptor sensor reveals rapid kinetics of allosteric modulation. *J Biol Chem* **285**(12):8793-8800.

Molinoff PB, Wolfe BB and Weiland GA (1981) Quantitative analysis of drug-receptor interactions: II. Determination of the properties of receptor subtypes. *Life Sci* **29**(5):427-443.

Nickerson M (1956) Receptor occupancy and tissue response. *Nature* **178**(4535):697-698.

Nikolaev VO, Hoffmann C, Bünemann M, Lohse MJ and Vilardaga JP (2006) Molecular basis of partial agonism at the neurotransmitter α_{2A}-adrenergic receptor and G_i-protein heterotrimer. *J Biol Chem* **281**(34):24506-24511.

Park J, Kile BM and Wightman RM (2009) In vivo voltammetric monitoring of norepinephrine release in the rat ventral bed nucleus of the stria terminalis and anteroventral thalamic nucleus. *Eur J Neurosci* **30**(11):2121-2133.

Park J, Takmakov P and Wightman RM (2011) In vivo comparison of norepinephrine and dopamine release in rat brain by simultaneous measurements with fast-scan cyclic voltammetry. *J Neurochem* **119**(5):932-944.

Philipp M and Hein L (2004) Adrenergic receptor knockout mice: distinct functions of 9 receptor subtypes. *Pharmacol Ther* **101**(1):65-74.

Philippu A and Matthaei H (1988) Transport and storage of catecholamines in vesicles. In: Trendelenburg U and Weiner N (eds.) Catecholamines. Handb. Exp. Pharmacol. Vol. 90/I, Springer (Berlin, Heidelberg), pp. 1-42.

Reiner S, Ambrosio M, Hoffmann C and Lohse MJ (2010) Differential signaling of the endogenous agonists at the β_2-adrenergic receptor. *J Biol Chem.* **285**(46):36188-36198.

Ruffolo RR, Jr. (1986) Spare α adrenoceptors in the peripheral circulation: excitation-contraction coupling. *Fed Proc* **45**(9):2341-2346.

Sallés J, Giraldo J and Badia A (1994) Analysis of agonism at functional prejunctional α_2-adrenoceptors of rat vas deferens using operational and null approaches. *Eur J Pharmacol* **258**(3):229-238.

Severne Y, Ijzerman A, Nerme V, Timmerman H and Vauquelin G (1987) Shallow agonist competition binding curves for β-adrenergic receptors: the role of tight agonist binding. *Mol Pharmacol* **31**(1):69-73.

Vilardaga JP, Bünemann M, Krasel C, Castro M and Lohse MJ (2003) Measurement of the millisecond activation switch of G protein-coupled receptors in living cells. *Nat Biotechnol* **21**(7):807-812.

Vilardaga JP, Steinmeyer R, Harms GS and Lohse MJ (2005) Molecular basis of inverse agonism in a G protein-coupled receptor. *Nat Chem Biol* **1**(1):25-28.

Weiland GA and Molinoff PB (1981) Quantitative analysis of drug-receptor interactions: I. Determination of kinetic and equilibrium properties. *Life Sci* **29**(4):313-330.

Zürn A, Zabel U, Vilardaga JP, Schindelin H, Lohse MJ and Hoffmann C (2009) Fluorescence resonance energy transfer analysis of α_{2A}-adrenergic receptor activation reveals distinct agonist-specific conformational changes. *Mol Pharmacol* **75**(3):534-541.

Molecular Pharmacology Fast Forward. Published on February 29, 2012 as DOI: 10.1124/mol.112.077693
This article has not been copyedited and formatted. The final version may differ from this version.

Footnotes

This work was supported by the Deutsche Forschungsgemeinschaft [SFB487] and the European Research Council [Advanced Grant “Topas”].

Molecular Pharmacology Fast Forward. Published on February 29, 2012 as DOI: 10.1124/mol.112.077693
This article has not been copyedited and formatted. The final version may differ from this version.

Figure legends

Figure 1. Schematic model of α_{2A}-AR$^{FlAsH/CFP}$ and $G_i^{CFP/YFP}$ sensors. (A) The α_{2A}-AR$^{FlAsH/CFP}$ sensor carries the donor fluorescent protein CFP at the C-terminus and the acceptor fluorophore FlasH into the third intracellular loop (*left*). FRET changes between the labels were determined after superfusion with the full agonist norepinephrine in single HEK-293 cells expressing the FRET-based receptor construct (*right*). The simultaneous decrease in FlAsH emission (F^*_{FlAsH}, yellow trace) and increase in CFP emission (F^*_{CFP}, blue trace) results in a significant decrease of the FRET ratio (F^*_{FlAsH}/F^*_{CFP}, red trace). (B) The $G_i^{CFP/YFP}$ sensor consists of the three subunits Gα-YFP, Gβ and Gγ-CFP (left). HEK-293 cells expressing the $G_i^{CFP/YFP}$ sensor showed a decrease of the FRET ratio (F^*_{YFP}/F^*_{CFP}, red trace) in response to the norepinephrine-dependent α_{2A}-AR activation (*right*).

Figure 2. Kinetics of α_{2A}-AR activation. Cells expressing the α_{2A}-AR$^{FlAsH/CFP}$ sensor were superfused with different norepinephrine concentrations. The fluorescence emissions F^*_{FlAsH} and F^*_{CFP} were recorded every 20 ms. (A) Relationship between norepinephrine concentrations and amplitudes of the FRET signals. The FRET changes were calculated as percentage of the change induced by norepinephrine 1 mM, which was assayed in each individual experiment as a reference. (B) Activation time constants are plotted as a function of norepinephrine concentration. Values were obtained from fitting the kinetic recordings with a monoexponential equation. For each norepinephrine concentration, data are means ± S.E. of 6-10 independent cells.

Molecular Pharmacology Fast Forward. Published on February 29, 2012 as DOI: 10.1124/mol.112.077693
This article has not been copyedited and formatted. The final version may differ from this version.

Figure 3. Concentration-response curves of α_{2A}-AR activation in non-equilibrium conditions and at steady state. The values corresponding to the FRET amplitudes recorded every 20 ms until the steady state was achieved were fitted by a sigmoidal concentration-response model thus generating 150 curves. To simplify the graph, only a selection of curves is shown and the corresponding EC_{50}-values are listed in Table 1.

Figure 4. Kinetics of G_i-activation. Single HEK-293 cells expressing the α_{2A}-AR and the trimeric $G_i^{CFP/YFP}$ sensor were superfused with different norepinephrine concentrations. The fluorescence emissions were recorded every 100 ms. (A) The graph shows the relationship between increasing concentrations of norepinephrine and the amplitude of the FRET signals. Similar to the data depicted in Fig. 2A, the FRET changes were calculated as percentage of the maximal response triggered by norepinephrine 1 mM at equilibrium, which was assayed in each individual experiment as a reference. (B) Activation time constants are shown as a function of norepinephrine concentration. Values were obtained from fitting the kinetic recordings with a monoexponential equation. At saturating concentrations of norepinephrine the speed of receptor-mediated G-protein activation was ~600 ms. For each norepinephrine concentration, data are means ± S.E. of 8-14 independent cells.

Figure 5. Concentration-response curves of G_i-activation in non-equilibrium conditions and at the steady state. The values corresponding to the FRET amplitudes recorded every 100 ms until the steady state was reached (Fig. 4) were fitted by a sigmoidal concentration-response model and plotted as a function of NE concentration. A

Molecular Pharmacology Fast Forward. Published on February 29, 2012 as DOI: 10.1124/mol.112.077693
This article has not been copyedited and formatted. The final version may differ from this version.

selection of the most significant curves is shown here and the corresponding EC_{50}-values listed in Table 2.

Figure 6. Potency and efficacy of norepinephrine-dependent α_{2A}-AR activation as a function of time. (A) The E_{max}-values resulting from α_{2A}-$AR^{FlAsH/CFP}$ activation were fitted by a monoexponential kinetic model (half-life ~60 ms), whereas the E_{max}-values characterizing $G_i^{CFP/YFP}$ activation followed a two-phase exponential kinetics (half-life$_1$ ~130 ms; half-life$_2$ ~ 660ms). (B) The calculated logEC_{50}-values resulting from the analysis of the concentration-response curves of α_{2A}-$AR^{FlAsH/CFP}$ or $G_i^{CFP/YFP}$ activation were fitted by one-phase exponential decay models and plotted as a function of time. (C) The relationship between the EC_{50}-values of norepinephrine required for receptor and G-protein activation was calculated as the ratio of the EC_{50}-values resulting from the analysis of the concentration-response curves depicted in Figure 3 and 5.

Molecular Pharmacology Fast Forward. Published on February 29, 2012 as DOI: 10.1124/mol.112.077693
This article has not been copyedited and formatted. The final version may differ from this version.

Table 1

Time-dependent norepinephrine potency of α_{2A}-AR$^{FlAsH/CFP}$ activation.

Time, ms	**EC_{50}, µM**	**95% CI, µM**
40	26.0	13.9 – 50.2
120	24.5	16.4 – 34.6
240	16.2	12.4 – 22.7
400	9.45	6.71 – 13.4
560	5.94	4.67 – 7.52
720	5.22	4.27 – 6.39
880	5.05	3.19 – 4.53
1040	3.41	2.75 – 4.24
1360	3.34	2.59 – 4.14
2000	2.51	1.99 – 3.08
2960	2.55	1.99 – 3.12

CI, confidence interval

Molecular Pharmacology Fast Forward. Published on February 29, 2012 as DOI: 10.1124/mol.112.077693
This article has not been copyedited and formatted. The final version may differ from this version.

Table 2

Time-dependent norepinephrine potency of α_{2A}-AR mediated $G_i^{CFP/YFP}$ activation

Time, s	**EC_{50}, nM**	**95% CI, µM**
0.5	103	23.4 – 451
1.0	77.0	24.6 – 281
1.5	73.2	28.9 – 221
2.0	59.8	31.6 - 153
3.0	45.3	25.4 – 102
4.0	25.9	13.8 – 52.8
5.0	20.2	9.82 – 39.6
10	10.1	5.23 – 17.5
15	9.10	3.01 – 13.2

CI, confidence interval

Fig. 1

A)

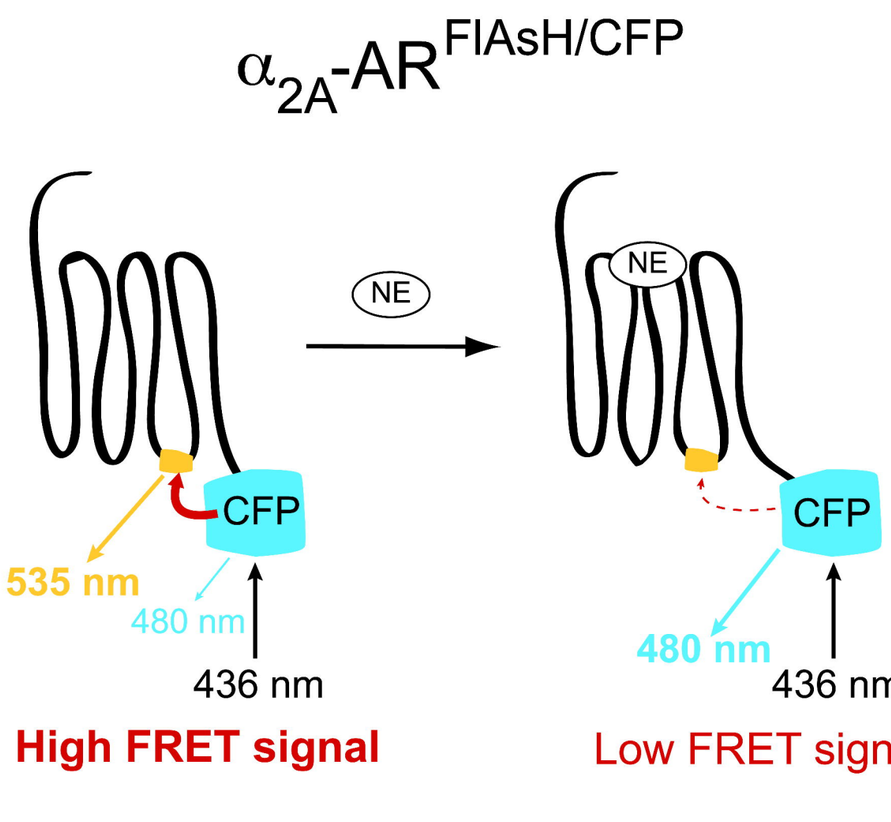

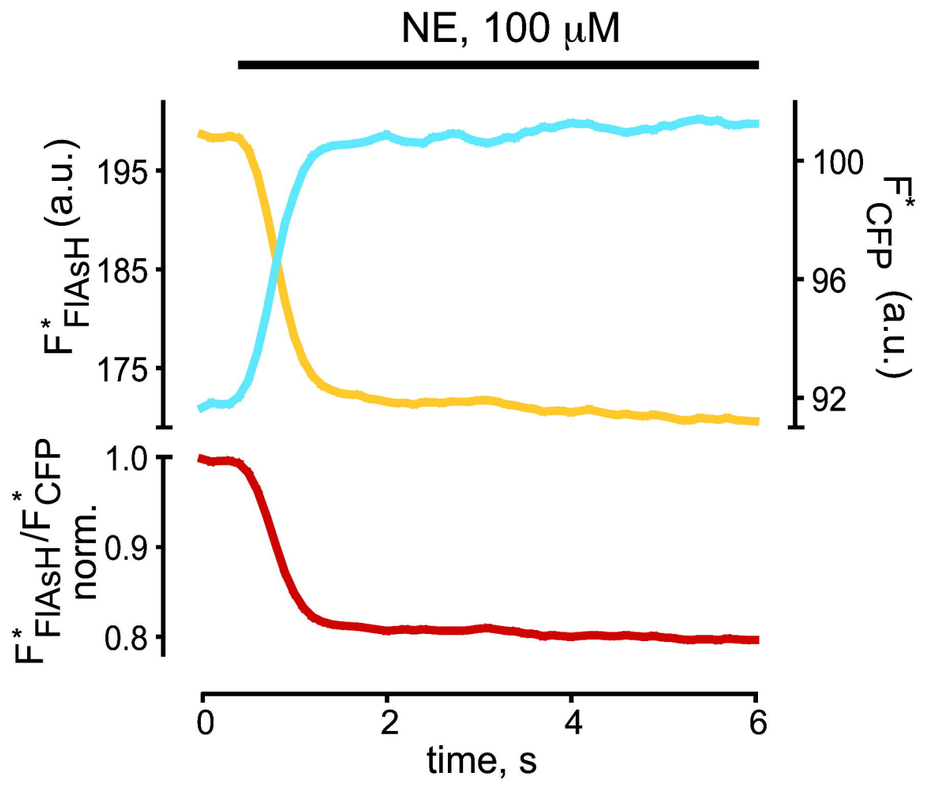

B)

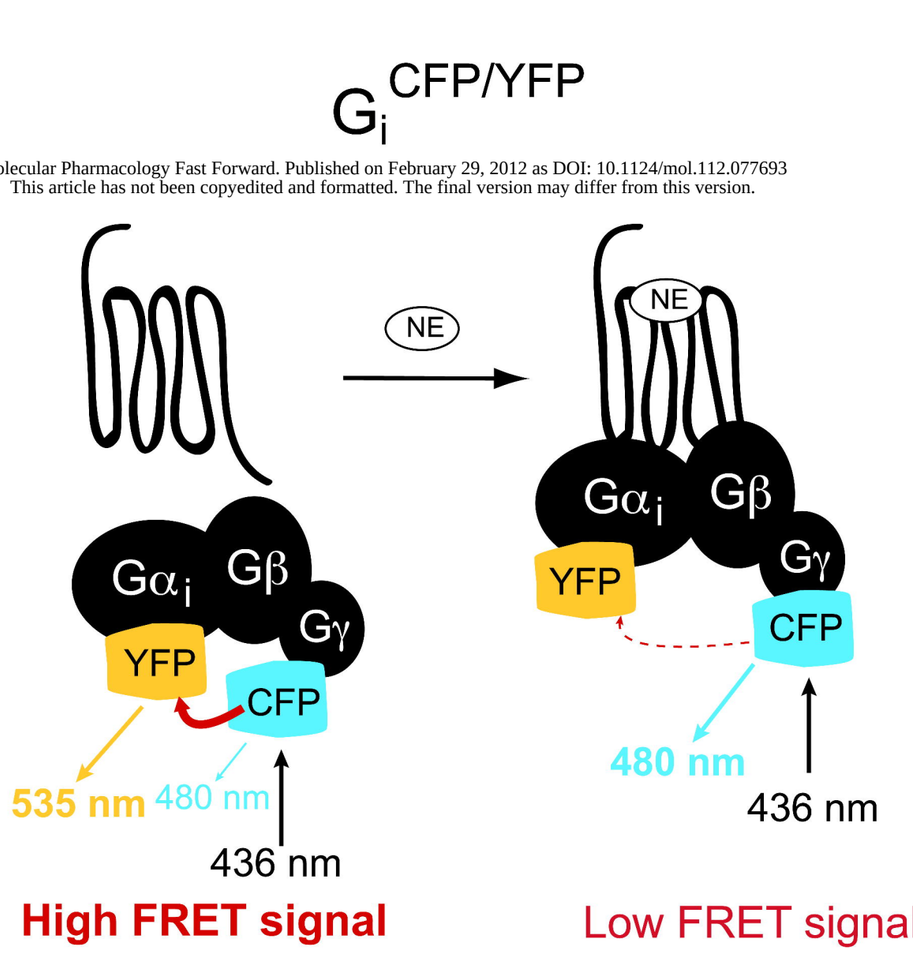

Molecular Pharmacology Fast Forward. Published on February 29, 2012 as DOI: 10.1124/mol.112.077693
This article has not been copyedited and formatted. The final version may differ from this version.

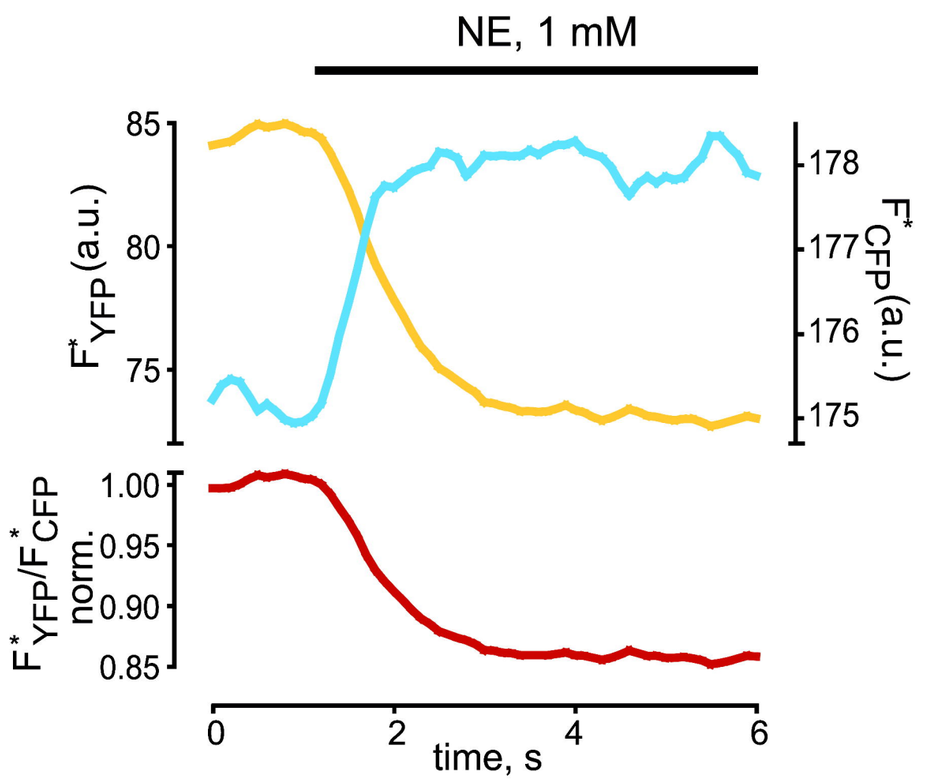

Molecular Pharmacology Fast Forward. Published on February 29, 2012 as DOI: 10.1124/mol.112.077693
This article has not been copyedited and formatted. The final version may differ from this version.

Fig. 2

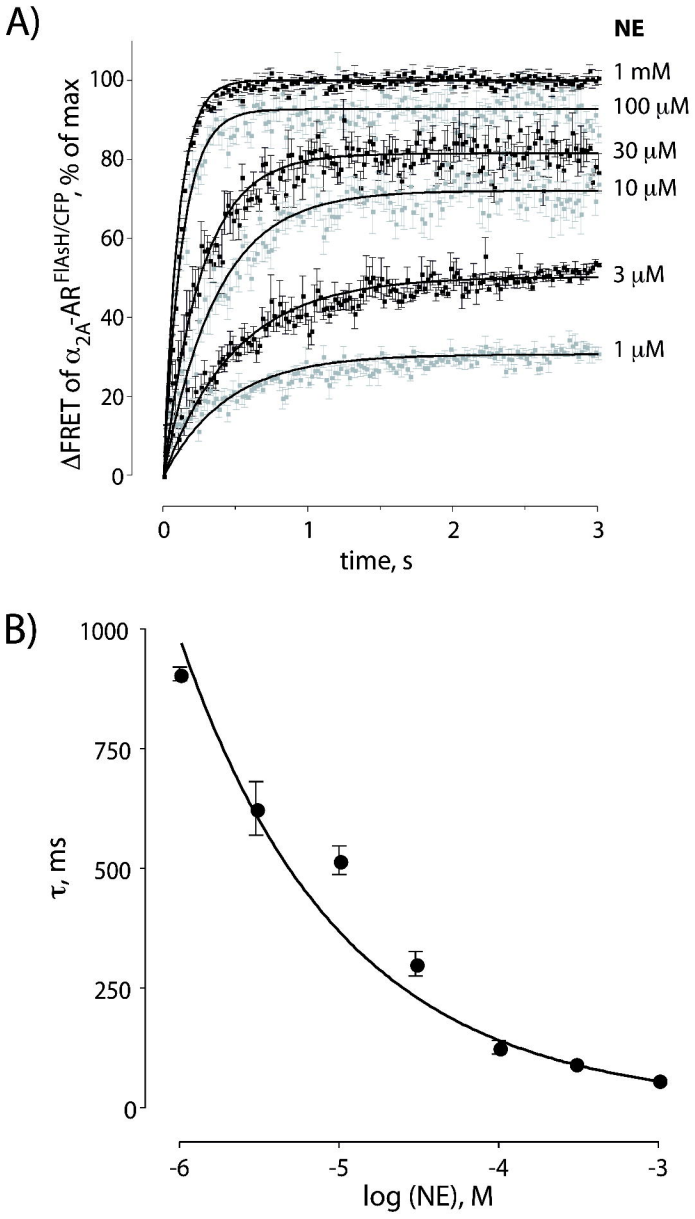

Molecular Pharmacology Fast Forward. Published on February 29, 2012 as DOI: 10.1124/mol.112.077693
This article has not been copyedited and formatted. The final version may differ from this version.

Fig. 3

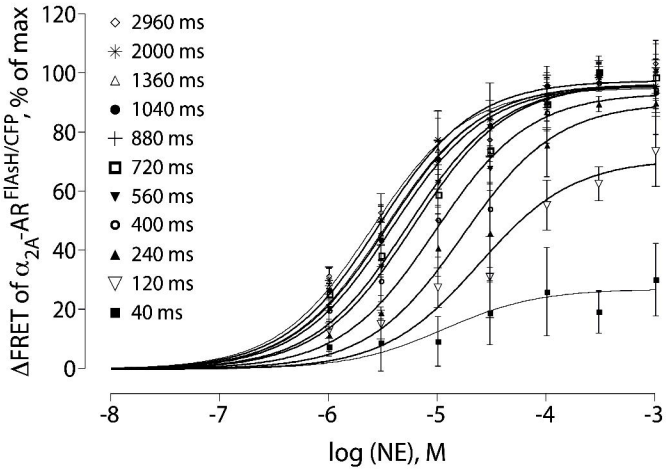

Molecular Pharmacology Fast Forward. Published on February 29, 2012 as DOI: 10.1124/mol.112.077693
This article has not been copyedited and formatted. The final version may differ from this version.

Fig. 4

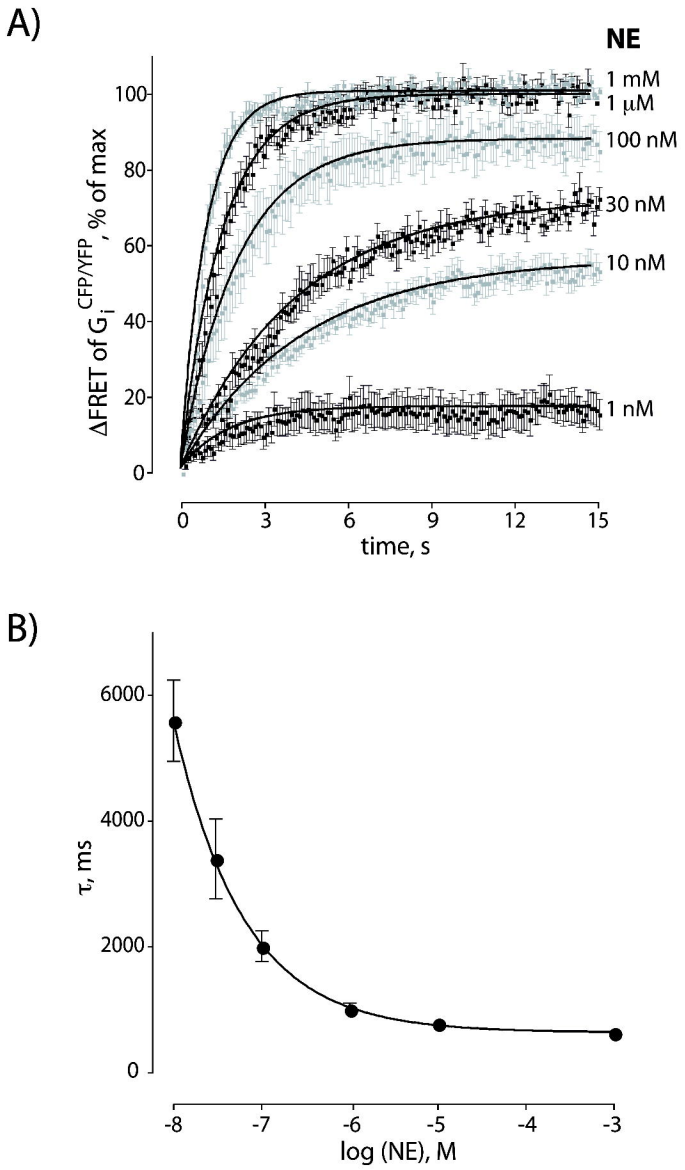

Molecular Pharmacology Fast Forward. Published on February 29, 2012 as DOI: 10.1124/mol.112.077693
This article has not been copyedited and formatted. The final version may differ from this version.

Fig. 5

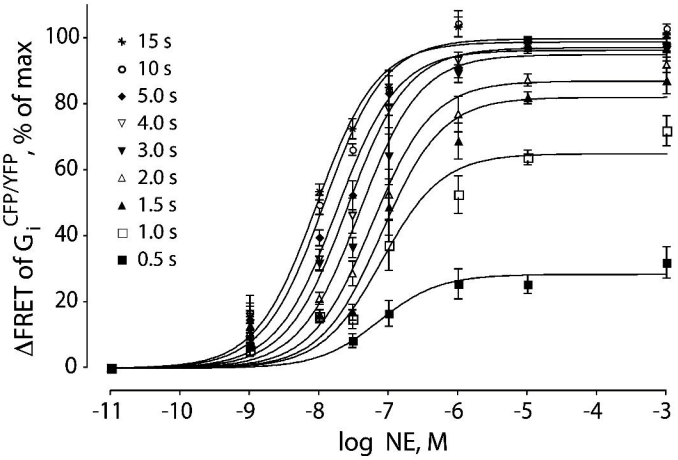

Molecular Pharmacology Fast Forward. Published on February 29, 2012 as DOI: 10.1124/mol.112.077693
This article has not been copyedited and formatted. The final version may differ from this version.

Fig. 6